Supporting information

Evolution of Hollow TiO_2 Nanostructures via the Kirkendall Effect Driven by Cation Exchange with Enhanced Photoelectrochemical Performance

Yanhao Yu,[1] Xin Yin,[1] Alexander Kvit,[1,2] Xudong Wang[1, *]

1. Department of Materials Science and Engineering, University of Wisconsin-Madison

2. Materials Science Center, University of Wisconsin-Madison

* Email: xudong@engr.wisc.edu

Experimental Details

(1) Pulsed vapor deposition setup and hollow TiO_2 structure evolution condition.

A home-made atomic layer deposition (ALD) system was used to carry out the pulsed vapor deposition of hollow TiO_2 nanostructures from ZnO NW templates. The target substrate was loaded on a quartz tube and placed at the position 5 cm away from the precursor inlet nozzle. N_2 gas with a flow rate of 40 sccm was introduced into the chamber to serve as the carrier gas. The system's base pressure was kept at 3.2 Torr. The hollow TiO_2 evolution and 3D TiO_2 nanorod (NR) growth were conducted under the same growth conditions. The chamber temperature was maintained at 600 ℃ during the entire growth process. $TiCl_4$ and H_2O vapors were pulsed into the deposition chamber separately with a pulsing time of 500ms and separated by 60s N_2 purging. Therefore, one deposition cycles involves 500 ms of H_2O pulse + 60s of N_2 purging + 500 ms of $TiCl_4$ pulse + 60 s of N_2 purging with a $TiCl_4$ pressure change of 110 millitorr (chamber pressure difference before and after ALD valve open). The chamber was cooled down naturally under N_2 flow after growth. To acquire different stages of nanostructure (Figure 1and 4, Figure S8 and S9),

deposition was terminated at the cycles of 2, 5, 10, 25, 50, 100, 200 and 400 and the samples were removed from the chamber for characterization.

(2) Control experimental details and polycrystalline film coating condition.

All control experiments and film coating were performed in the same ALD system and under identical conditions as described above except precursor supply and temperature adjustments. In the control experiments of surface reaction study, three precursor and temperature compositions was applied: 10 cycles of $TiCl_4$ pulse without H_2O supply at 600 ℃, 10 cycles of $TiCl_4$ pulse without H_2O supply at 300 ℃, and 10 cycles of H_2O pulse without $TiCl_4$ supply at 600 ℃. To study the ZnO diffusion effect, a conformal amorphous TiO_2 thin film was coated on the ZnO nanowire (NW) by 200-cycle ALD at 100 ℃. As soon as the coating was finished, without cooling down the chamber and taking out the sample, the chamber temperature was directly raised to 600 ℃ and annealed the sample at this temperature for 10 hours under N_2 flow. To coat the ZnO NWs with polycrystalline TiO_2 films for PEC performance comparison, the deposition temperature was set at 300 ℃ and 400 cycles and 800 cycles of ALD growth were applied.

(3) Hydrothermal growth and chemical vapor deposition of ZnO nanostructure.

The straight ZnO NW arranges were growth by the hydrothermal method, following the previously reported procedure.[1] A thin film of ZnO seeds was deposited onto fluorine doped tin oxide (FTO) conductive glass substrate by dropping 5 mM zinc acetate solution and baking for 20 minutes at 300 °C. After that, the substrate with seeds was immersed in the nutrient solution with the seeds surface facing downward. The nutrient solution consisted 25 mM zinc nitrate and 25 mM hexamethylenetetramine (HMT). After 6 hour growth at 90 °C, FTO substrate was taken out from nutrient solution, washed by DI water and dried in the air. The plate-caped ZnO NWs and 3D ZnO nanosheets were synthesized by Chemical vapor deposition. Pure ZnO powder was used as the precursor and located at the center of the furnace. Polycrystalline alumina substrates were placed downstream in the furnace. The system was kept at a low pressure (~50 Pa). 50 sccm argon and 5 sccm oxygen were used as the carrier gas. The system was heated to 1000 °C during the first 40 minutes and reached 1300 ℃ after another 40 minutes. Subsequently, the system was cooled down to room temperature naturally. The 3D ZnO nanosheets (Figure S6) were acquired at the chamber temperature of 1200 ℃.

(4) Characterization. SEM measurements were performed on Zeiss Leo 1530 field- emission microscopes and TEM measurements were done on FEI TF30 and Titan microscopes. Scanning transmission electron microscopy (STEM) experiments were performed on a FEI Titan microscope with a CEOS probe aberration-corrector operated at 200 keV. STEM images were collected with a 24.5 mrad probe semi-angle, 25 pA probe current, and STEM resolution of 0.8 ÅA. STEM electron energy loss spectroscopy (EELS) spectrum images (SIs) were acquired using a 24.5 mrad probe semi-angle, spectrometer collection angle of 102 mrad, 100 196 pA probe current, and STEM resolution of 2.1A1.55 Å. Energy dispersive spectroscopy (EDS) measurements were done at probe current 400 390 pA. Short exposure time (500 ms) used to avoid sample damaging artifacts during EDS SI. The samples were tested for damaging after SI. EDS results on Figure S6d and S7e were performed on SEM LEO 1530. X-ray diffraction pattern were acquired from the Bruker D8 Discovery with Cu Kα radiation.

(5) PEC measurements.

Prior to integrated to PEC system, the as-synthesized TiO_2 nanostructures were covered by an additional layer of polycrystalline anatase TiO_2 film deposited by 400 cycles of ALD to prevent the contact between FTO surface and electrolyte. A typical three-electrode electrochemical cell setup was applied to carry out the PEC characterization with 3D hollow TiO_2 nanoforest as the working electrode, Pt wire as the counter electrode and a saturated calomel electrode (SCE) as the reference electrode. All electrodes were emerged in a 1 M KOH electrolyte and working electrode was illuminated by a light source with intensity of 100 mW/cm^2 provided by a 150 W Xenon lamp.

Reference:

(1) Wang, F.; Seo, J. H.; Bayerl, D.; Shi, J.; Mi, H.; Ma, Z.; Zhao, D.; Shuai, Y.; Zhou, W.; Wang, X. D. *Nanotechnology* **2011**, *22*, 225602.

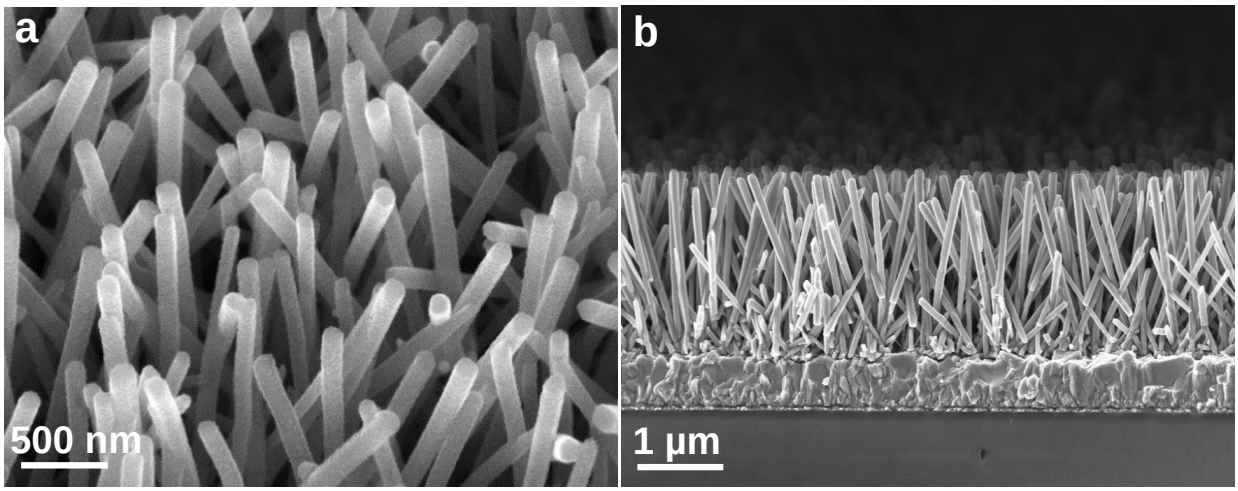

Figure S1. SEM images of **(a)** ZnO NWs after 2 cycles of deposition; and **(b)** the cross section of ZnO NW template with a length ~2 µm.

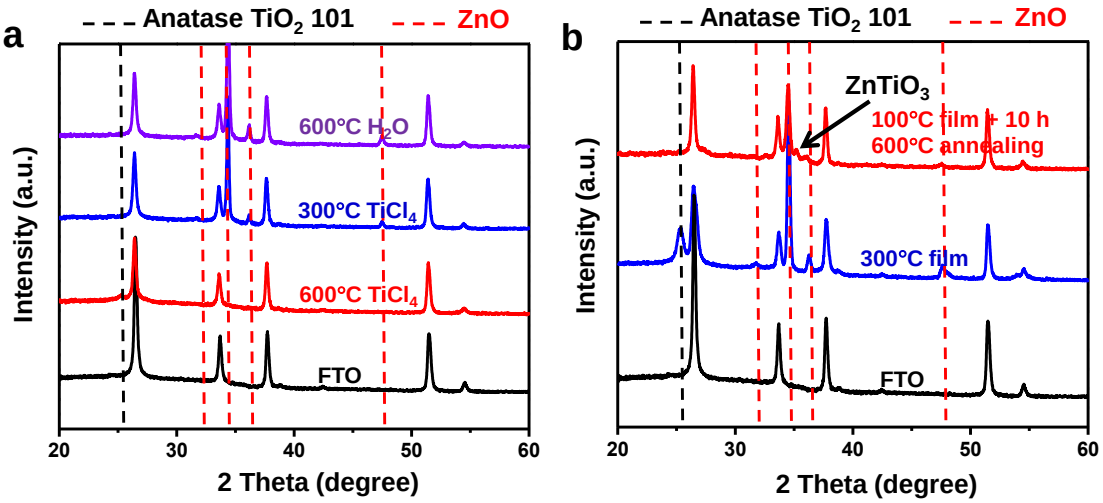

Figure S2. (a) X-ray diffraction (XRD) pattern of ZnO NW samples after 10 cycles of $TiCl_4$ pulses without H_2O supply at 600 ℃ (red); 10 cycles of $TiCl_4$ pulse without H_2O supply at 300 ℃ (blue); and 10 cycles of H_2O pulse without $TiCl_4$ supply at 600 ℃ (purple). **(b)** XRD of $ZnTiO_3$/ZnO core/shell structure fabricated via 200 cycles of ALD TiO_2 coating on ZnO NWs at 100 ℃ followed by 10 hours annealing at 600 ℃. The spectrum of a 300-cycle ALD TiO_2 film deposited at 300 °C on ZnO NWs without annealing is included for reference (blue).

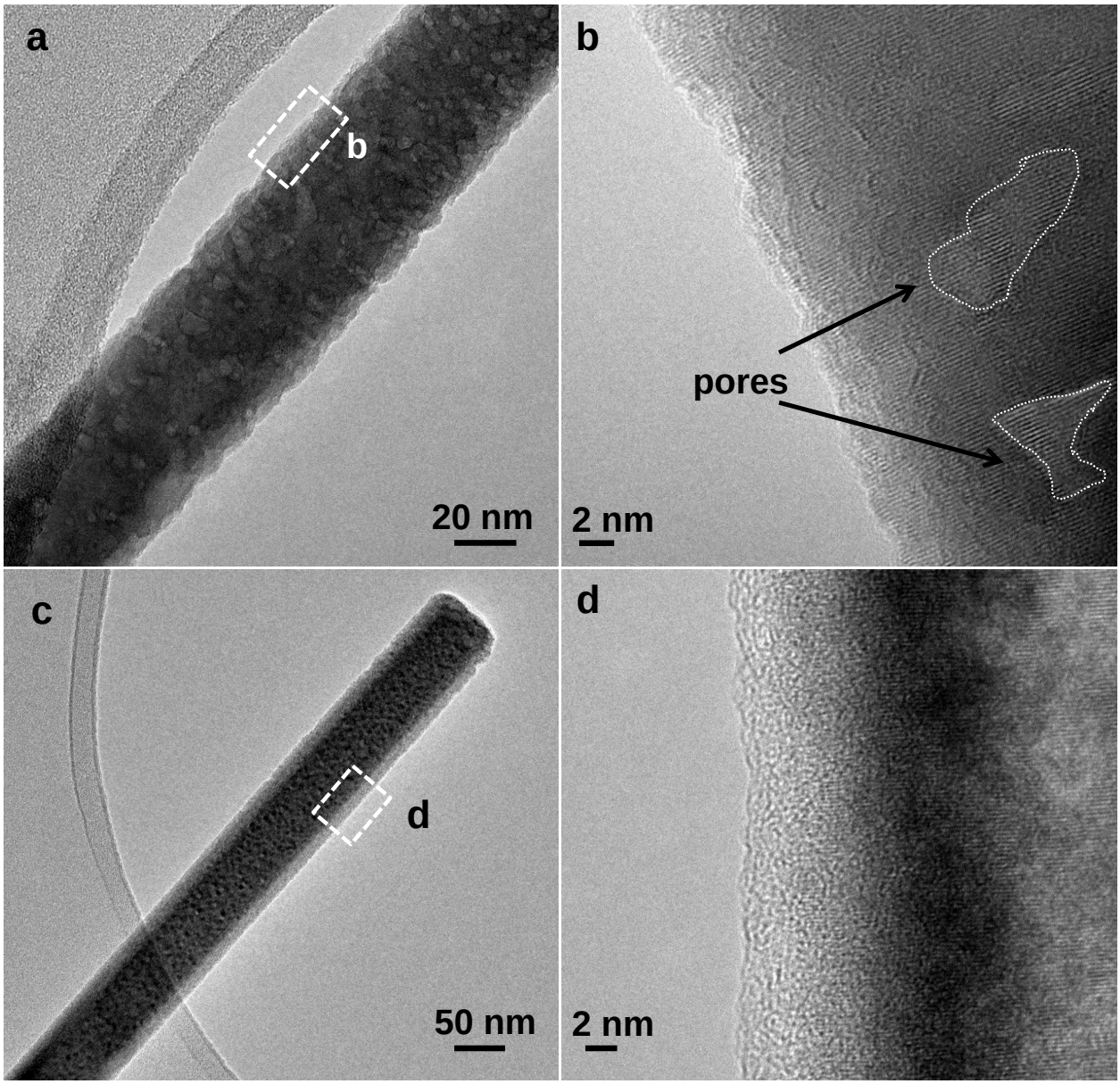

Figure S3. (a,b) TEM images of a ZnO NW after 10 cycles of H_2O pulse without $TiCl_4$ supply at 600 ℃, exhibiting a clear ZnO lattice with defect pores located on the NW surfaces. **(c,d)** TEM images of a ZnO NW after 10 cycles of $TiCl_4$ pulse without H_2O supply at 300 ℃, showing the ZnO lattice in the center region with an amorphous film TiO_2 film on the surface.

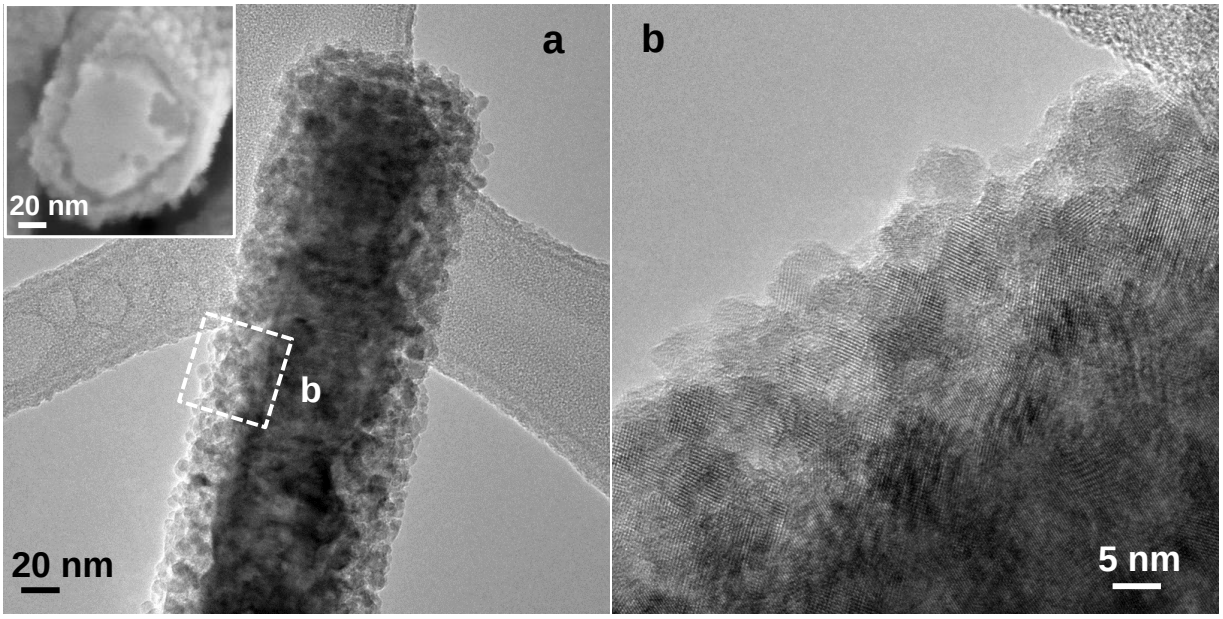

Figure S4. TiO_2/ZnO core-shell structure formed by 5 second continuous $TiCl_4$ exposure at 600 °C.

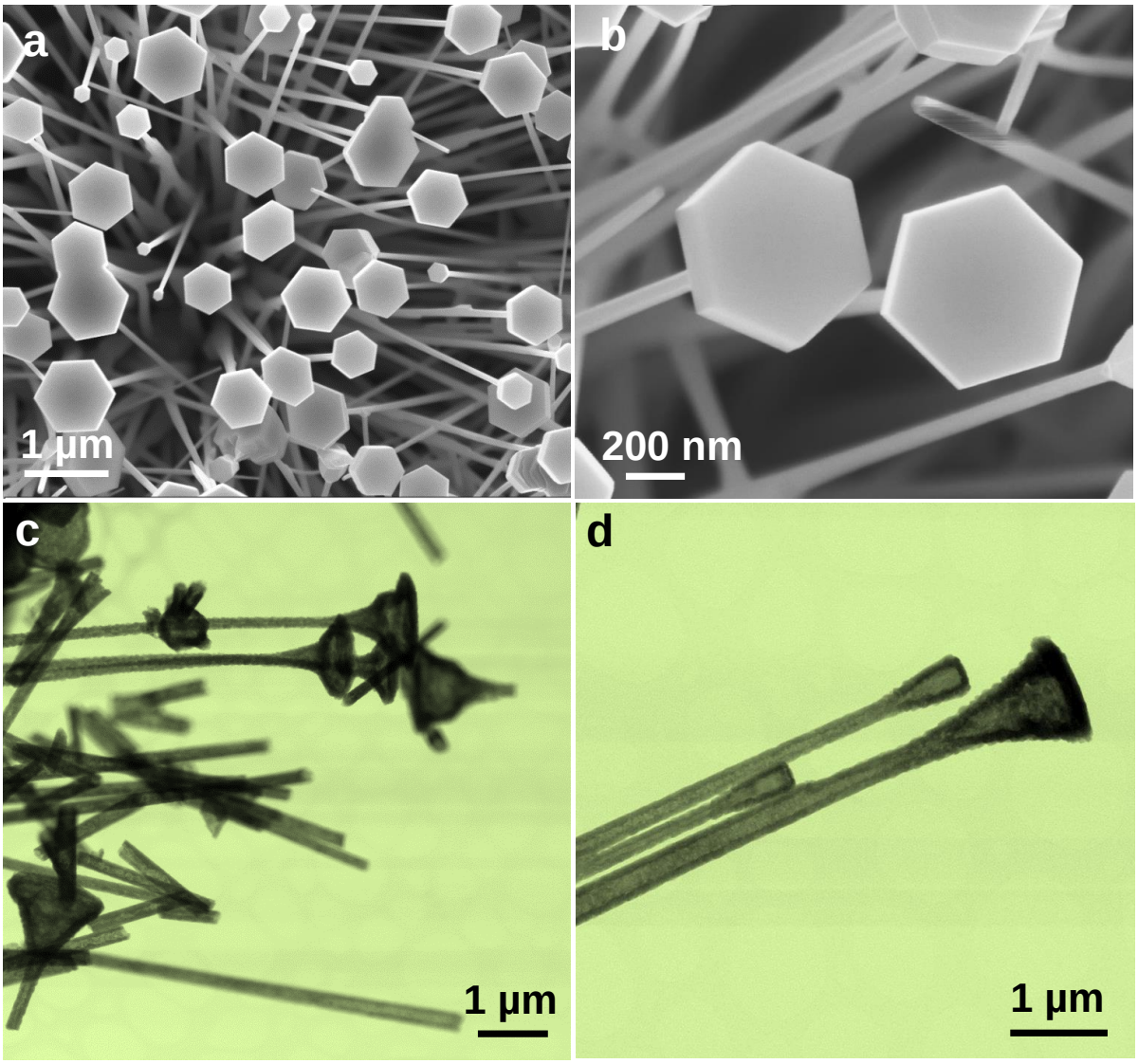

Figure S5. (a,b) Plate-caped ZnO NW bundles produced by chemical vapor deposition at 1300 °C. **(c,d)** Bright field STEM images of the plate-caped NW structure after 300 cycles **(c)** and 600 cycles **(d)** of $TiCl_4$ deposition, demonstrating the precisely preserved morphology and hollow feature.

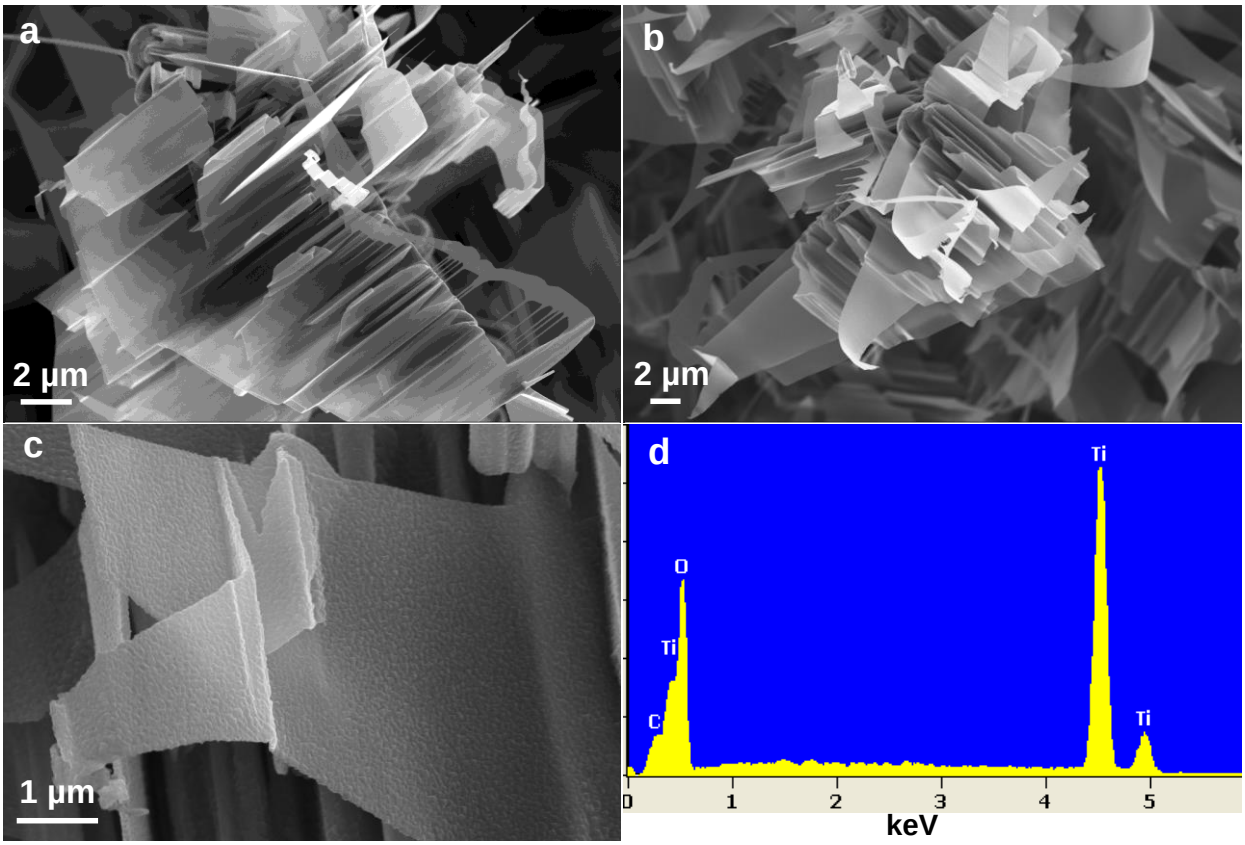

Figure S6. Demonstration of the universal capability of morphology duplication. **(a)** SEM image of large-area 3D-interconnected ZnO nanosheet structure. **(b)** TiO_2 hollow structure created by 400 cycles of deposition. **(c)** Higher magnification SEM image showing the surface feature of a TiO_2 sheet replica. **(d)** EDS acquired from the replicated structure reveals the pure TiO_2 composition.

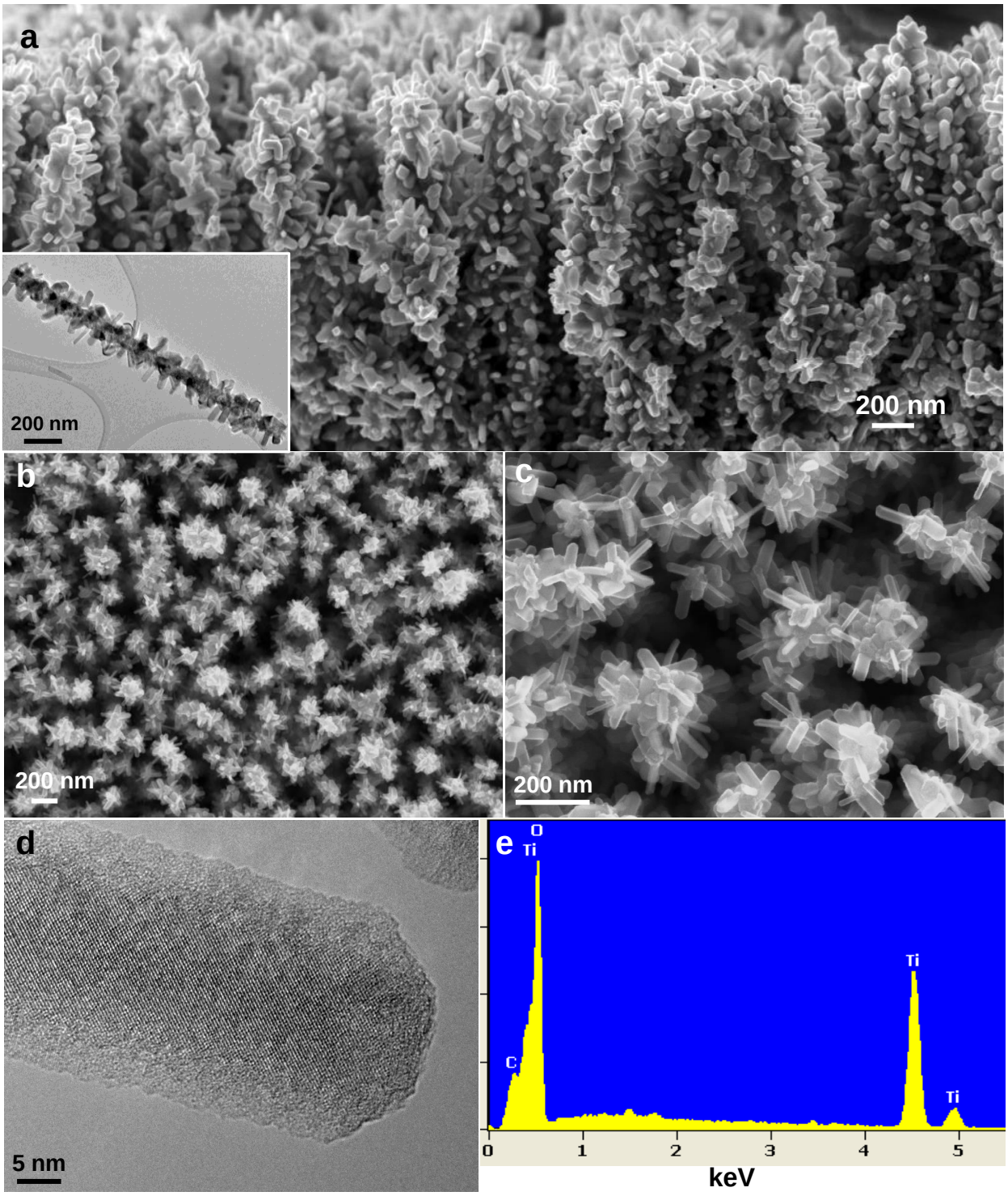

Figure S7. SEM images of **(a)** cross-sectional view and **(b, c)** top view of 3D TiO_2 nanoforest. Inset of (a) is the TEM image of a single branched TiO_2 NW. **(d)** High resolution TEM image of the TiO_2 branch revealing its single crystalline feature. **(e)** EDS obtained from the TiO_2 nanoforest confirming the pure TiO_2 composition.

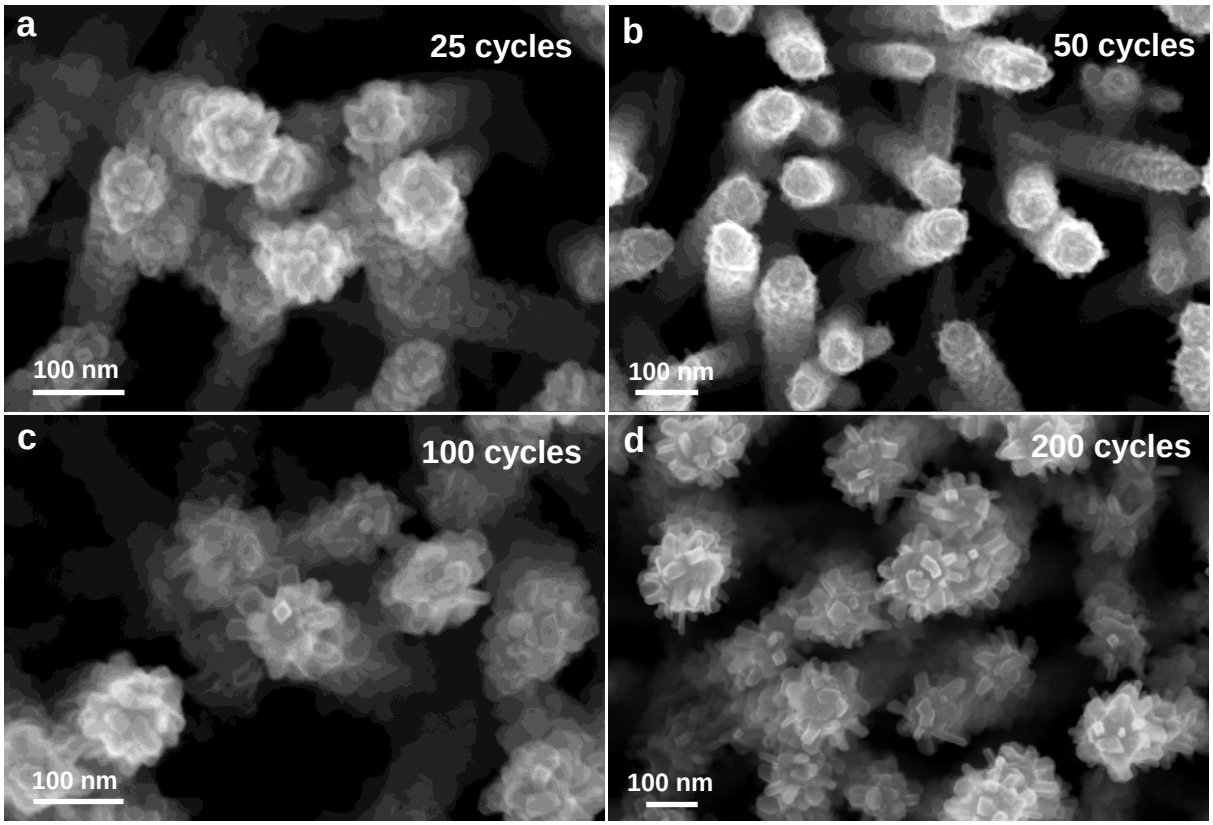

Figure S8. SEM observation of TiO_2 NRs growth process via SPCVD. Aspect ratio of the branch increases following the deposition cycles: 25 cycles **(a)**, 50 cycles **(b)**, 100 cycles **(c)**, 200 cycles **(d)**.

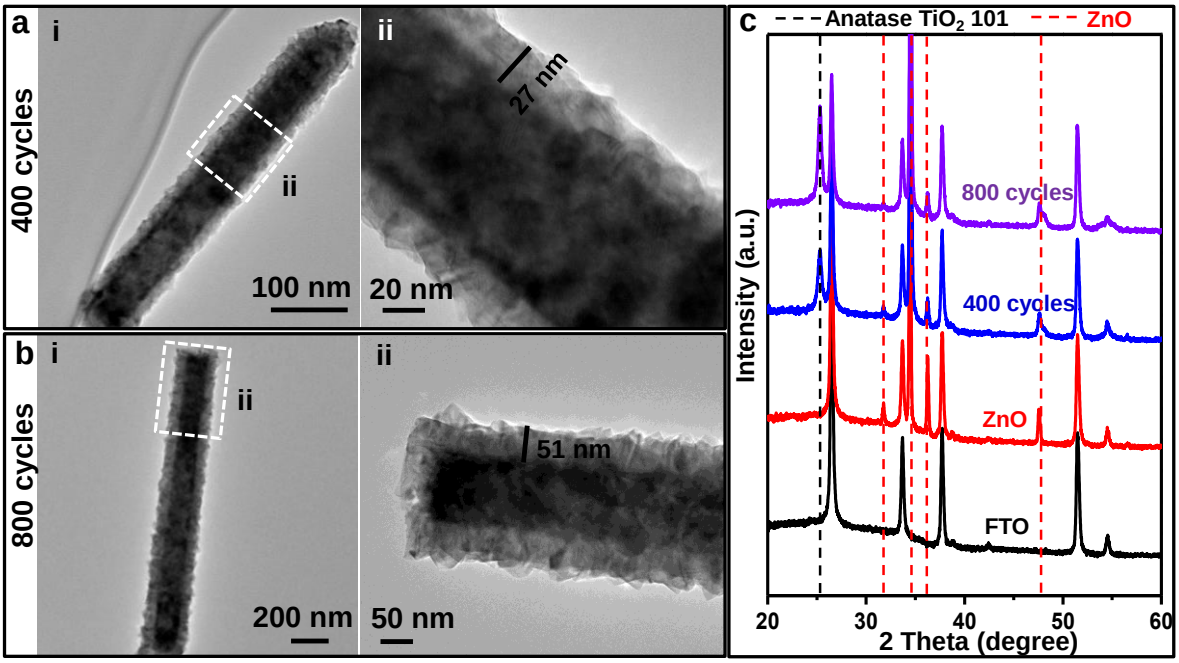

Figure S9. TEM images of TiO_2/ZnO core-shell NW structure, where the TiO_2 shells were deposited by 400 cycles **(a)** and 800 cycles **(b)** of ALD. **(c)** XRD results of corresponding samples confirming the ZnO and anatase TiO_2 phases.